Modeling the Tungsten Sites of Inactive and Active Forms of Hyperthermophilic *Pyrococcus furiosus* Aldehyde Ferredoxin Oxidoreductase

Samar K. Das, Dulali Biswas, Rabindranath Maiti, and Sabyasachi Sarkar*

Contribution from the Department of Chemistry, Indian Institute of Technology, Kanpur, Kanpur-208016, India

Received April 10, 1995[⊗]

Abstract: The complex $[Et_4N]_2[W^{VI}O_2(mnt)_2]$ (**1**), $[Et_4N]_2[W^{IV}O(mnt)_2]$ (**2**), and $[Et_4N]_2[W^{VI}O(S_2)(mnt)_2]$ (**3**) (mnt^{2-} = 1,2-dicyanoethylenedithiolate) have been synthesized as possible models for the tungsten cofactor of inactive red tungsten protein (RTP) and the active aldehyde ferredoxin oxidoreductase (AOR) of the hyperthermophilic archaeon *Pyrococcus furiosus*. The $[Ph_4P]^+$ salt of the complex anion of **1**·$2H_2O$ crystallizes in space group *Pbcn*, with a = 20.526(3) Å, b = 15.791(3) Å, c = 17.641(3) Å, and Z = 4. The $W^{VI}O_2S_4$ core of $[Ph_4P]_2[W^{VI}O_2(mnt)_2]$·$2H_2O$ has distorted octahedral geometry with *cis* dioxo groups. **2** crystallizes in space group $P2_12_12$, with a = 14.78(3) Å, b = 30.08(2) Å, c = 7.37(4) Å, and Z = 4. The complex anion of **2** has a distorted square-pyramidal structure with an axial W═O bond. **3** crystallizes in space group $P2_1/a$, with a = 12.238(3) Å, b = 18.873(2) Å, c = 15.026(2) Å, β = 102.84(2)°, and Z = 4. The anion of **3** with a terminal oxo group and a *dihapto* disulfido ligand in an adjacent position is the first example of a seven-coordinate W(VI) species with bis-dithiolene coordination. The complexes **1**−**3** have been characterized by IR, UV−visible, ^{13}C NMR, negative ion FAB mass spectra, and electrochemical properties. Complex **1** reacts with H_2S, PhSH, 1,4-dithiothreitol (DTT), or dithionite ($S_2O_4^{2-}$) to yield **2** with the oxidation of these reducing agents suggesting intramolecular electron transfer in the respective intermediates across the W(VI)−sulfur bond. Participation of this type of redox reaction, seemingly unrealistic from the point of view of real reduction potential values of **1** and of these reductants, is best explained by the formation of a precursor complex. This relates to the essential formation of a Michaelis (enzyme−substrate) complex wherein the individual chemical identity of the free enzyme and unbound substrate is lost. Subsequent atom transfer reaction embodies internal electron transfer between the two redox partners present in the enzyme−substrate complex. The terminal oxo group of **2** is readily protonated (pH < 4) to yield $[W^{IV}(mnt)_3]^{2-}$. **2** responds to a metal exchange reaction with MoO_4^{2-} to form $[Mo^{IV}O(mnt)_2]^{2-}$ which is similar to *in vitro* reconstitution of the molybdenum cofactor by MoO_4^{2-} in tungsten formate dehydrogenase (W-FDH). The model reaction between **2** and MoO_4^{2-} involves a stepwise one-electron transfer reaction from W(IV) to Mo(VI) with the intermediate formation of EPR active W(V) species. Oxidative addition of elemental sulfur from **2** affords **3**, which gives sulfur atom transfer reactions with several thiophiles. **3** reacts with Ph_3P in a second-order process (A + 2B type) to yield **2** and Ph_3PS with the observed rate constant k_2 = 4.3 (± 0.06) M^{-1} s^{-1} at 25 °C ($\Delta H^{\ddagger}$ = 5.14 (± 0.46) kcal/mol, $\Delta S^{\ddagger}$ = −38.35 (± 1.5) cal/(deg·mol)). A cyclic voltammetric study suggests the attack of Ph_3P across the W−S bond in the WS_2 moiety of **3**. **2** catalyzes the reactions $Ph_3P + S \rightarrow Ph_3PS$ and $H_2 + S \rightarrow H_2S$, demonstrating its sulfur reductase activity. No such reaction is observed in the absence of **2**. Formaldehyde reduces **3** to **2**. Crotonaldehyde reacts with **3** to yield **2** and crotonic acid in MeCN containing H_2O (5% v/v) or in CH_2Cl_2 medium which demonstrates that aldehyde oxidase activity of **3** is similar to that of the active AOR enzyme of *P. furiosus*.

Introduction

The hyperthermophilic archaea (formerly archaeobacteria) that thrive at high temperature (∼100 °C) near undersea hydrothermal vents are considered to be the most primitive organisms on earth.[1] One of the best studied of these archaeons, *Pyrococcus furiosus*, contains the tungsten protein aldehyde ferredoxin oxidoreductase (AOR) and formaldehyde ferredoxin oxidoreductase (FOR).[2] These tungstoenzymes catalyze atom transfer reaction 1 with the proposed involvement of W(VI) as

$$RCHO + H_2O \rightleftharpoons RCOOH + 2H^+ + 2e^- \qquad (1)$$

the catalytic center for the oxidation of aliphatic aldehydes. The reduced W(IV) so formed is oxidized back to W(VI) by ferredoxin centers *via* FeS clusters. This back-reaction from W(IV) to W(VI) involves two one-electron processes with the elements of water being used as the source of the additional oxygen atom of the carboxylic acid.[2] The intermediate W(V) involved in the regeneration stage of the catalytic cycle has not yet been identified by EPR spectroscopy.

In the purification procedure of AOR, an inactive "red tungsten−iron−sulfur protein (RTP)" has also been isolated.[2] The difference between the active AOR and inactive RTP forms has been speculated to be the presence of a susceptible W−SH moiety in the former and a W═O group in the latter.[2b] This is similar to xanthine oxidase wherein the active sulfido form is

[⊗] Abstract published in *Advance ACS Abstracts,* January 15, 1996.

(1) Woeses, C. R.; Kandler, O.; Wheelis, M. L. *Proc. Natl. Acad. Sci. U.S.A.* **1990**, *87*, 4576. (b) Stetter, K. O. *Nature* **1982**, *300*, 258. (c) Stetter, K. O. In *The Thermophiles, General, Molecular and Applied Microbiology*; Brock, T. D., Ed.; John Wiley: New York, 1986; p 39. (d) Kelly, R. M.; Demming, J. N. *Biotechnol. Prog.* **1988**, *4*, 47. (e) Stetter, K. O.; Fiala, G.; Huber, R.; Segerer, G. *FEMS Microbiol. Rev.* **1990**, *75*, 117.

(2) (a) Bryant, F. O.; Adams, M. W. W. *J. Biol. Chem.* **1989**, *264*, 507. (b) Mukund, S.; Adams, M. W. W. *J. Biol. Chem.* **1993**, *268*, 13592; **1990**, *265*, 11508; **1991**, *266*, 14208. (c) Adams, M. W. W. *Adv. Inorg. Chem.* **1992**, *38*, 341. (d) Adams, M. W. W. *Annu. Rev. Microbiol.* **1993**, *47*, 627. (e) Adams, M. W. W. In *Encyclopedia of Inorganic Chemistry*; King, R. B., Ed.; John Wiley: Chichester, U. K., 1994; p 4284.

0002-7863/96/1518-1387$12.00/0

contaminated with inactive oxo form.[3] Interestingly, *P. furiosus* reduces available sulfur in the growth medium to H_2S in an apparently energy conserving reaction that disposes of molecular H_2 produced from the fermentation of carbohydrates.[4]

All of these tungstoenzymes have been shown to contain molybdopterin, a ligand of the metal in the cofactor, similar to that of oxomolybdoenzymes present in bacteria and eucarya.[5] The EXAFS results of sulfite oxidase are comparable to those for the tungsten site of RTP from *P. furiosus*, suggesting the presence of a dioxotungsten(VI) moiety with dithiolene coordination in RTP.[6]

The other tungstoenzymes which also contain molybdopterin ligation are carboxylic acid reductase (CAR),[7] formylmethanofuran dehydrogenase (FMDHII),[8] and tungsten formate dehydrogenase (W-FDH).[9] Among these, only W-FDH has been characterized by EXAFS studies.[9] The recent report of X-ray structure of *P. furiosus* AOR enzyme demonstrates the coordination of tungsten with two dithiolenes from two molybdopterin units.[10]

At this stage, the analogue model compounds of the hyperthermophilic tungstoenzymes demand that (i) the mononuclear oxotungsten complex should be coordinated by two dithiolene ligands, (ii) the chemistry of these systems under sulfiding conditions should help to understand the important relationship between active AOR and inactive RTP forms with the characterization of the related sulfido species, (iii) the stoichiometric and catalytic atom transfer reactions of these complexes interconvert the oxidized W(VI) and reduced W(IV) species in both directions, and (iv) the dinucleation of the tungsten center from the mononuclear complex is prevented during the course of reaction, a common feature of the abiological chemistry of tungsten and molybdenum complexes.[11] To understand the fundamental chemistry underlying enzymatic reactions of tungstoenzymes, it is necessary to synthesize well-characterized tungsten complexes that are capable of meeting the above criteria. The chemistry of oxotungsten(IV) complexes with sulfur donor ligands has not been explored to the same extent as for the corresponding oxomolybdenum(IV) complexes. This is due to the difficulty in reducing W(VI) species to W(IV) species. On the basis of W-EXAFS results of the dithionite-reduced tungstoformate dehydrogenase, the synthesis of $\{HB(Me_2pz)_3\}W^{IV}(SePh)\{S_2C_2(Ph)(2\text{-quinoxalinyl})\}$ [$HB(Me_2pz)_3$ = hydrotris(3,5-dimethylpyrazol-1-yl)borate] has been reported.[12] Nakamura and co-workers have structurally characterized bis(benzene-1,2-dithiolato) complexes of oxotungsten(VI, V, IV) using trimethylamine *N*-oxide and benzoin as the model substrates in relevance to the W-EXAFS results of the RTP protein.[13] However, these complexes show redox reactivities almost identical to those of the corresponding molybdenum complexes.[13] The other examples of hexacoordinated dioxotungsten(VI) complexes relevant to W−enzyme systems are $WO_2(R_2dtc)_2$ (R = Et, Me),[14a] $WO_2(pipdtc)_2$,[14a,b] and $[NH_4]_2[W^{VI}O_2(O_2CC(S)Ph_2)_2]$.[14c] The synthesis of a Schiff base complex like WO_2(ssp) (ssp = 2-(salicylideneamino)benzenethiolate(2−)) has been reported.[14b] The tungsten disulfur complexes $WX(S_2)(S_2CNR_2)$ (X = O, S; R = Me, Et) are known, but their reactivity is not described.[15] Some oxygen atom transfer reactions using tungsten complexes have been reported, and in the case of W(VI), the reactions lead to the formation of a W(V) dimer.[14b] Some W(IV) complexes have been shown to be avid oxygen acceptors.[16]

Experiments on the activation of *nit-1* nitrate reductase by W-FDH showed that molybdenum can displace tungsten from cofactor complex having dithiolene ligation when it was not bound to the protein.[9] Thus, it would be of interest as a model study if similar extrusion of dithiolenes from tungsten complexes by molybdate could be done. Here we describe our current chemical approach to address these problems. The synthesis and structural characterization of $[W^{VI}O_2(mnt)_2]^{2-}$ (**1**), $[W^{IV}O(mnt)_2]^{2-}$ (**2**), and $[W^{VI}O(S_2)(mnt)_2]^{2-}$ (**3**) and several of their pertinent properties addressing the reactions executed by tungstoenzymes are presented here. We also describe the reaction between **2** and MoO_4^{2-} to yield $[Mo^{IV}O(mnt)_2]^{2-}$, which is similar to extrusion of molybdopterin ligation of W-FDH by molybdate. The stoichiometric and catalytic sulfur atom transfer reactions of these complexes are demonstrated. A preliminary report of a part of this work in relevance to W-FDH has previously been provided.[17]

Experimental Section

Materials and Methods. Anaerobic syntheses and reactions were carried out in inert atmosphere using purified argon or under H_2S and in deoxygenated solvents. Na_2mnt ($mnt^{2-} = S_2C_2(CN)_2^{2-}$ = 1,2-dicyanoethylenedithiolate) was prepared by the method of Stiefel et al.[18]

Elemental analyses were determined with a EA 1108 elemental analyzer. Sulfur estimation was carried out by peroxide fusion of the complexes. After being leached with water and acidification, the precipitated tungstic acid was digested in a water bath to facilitate filtration, and from the filtrate, sulfate was estimated gravimetrically as $BaSO_4$. Infrared spectra were recorded as CsI pellets on Perkin Elmer 577 and FT 1600 series IR spectrophotometers. Electronic spectra were measured by a Shimadzu 160 spectrophotometer. ^{13}C NMR (100 MHz) spectra were obtained on a Bruker WM-400 FT NMR spectrometer using DMSO-d_6. Tetramethylsilane was used as an internal standard. Negative ion FAB mass spectra were taken in 3-nitrobenzyl alcohol by using a JEOL SX 102 DA-6000 mass spectrometer data system with an argon gun, operated at 6 kV and 10 mA. EPR spectra were obtained with a Varian E-109 spectrometer. Room-temperature solution spectra were obtained with a flat cell. EPR

(3) Bray, R. C. *Adv. Enzymol. Relat. Areas Mol. Biol.* **1980**, *51*, 107. (b) Bray, R. C. *Q. Rev. Biophys.* **1988**, *21*, 299.

(4) (a) Fiala, G.; Stetter, K. O. *Arch. Microbiol.* **1986**, *145*, 56. (b) Schicho, R. N.; Ma, K.; Adams, M. W. W.; Kelly, R. M. *J. Bacteriol.* **1993**, *175*, 1823. (c) Ma, K.; Schicho, R. N.; Kelly, R. M.; Adams, M. W. W. *Proc. Natl. Acad. Sci. U.S.A.* **1993**, *90*, 5341.

(5) Johnson, J. L.; Rajagopalan, K. V.; Mukund, S.; Adams, M. W. W. *J. Biol. Chem.* **1993**, *268*, 4848.

(6) George, G. N.; Prince, R. C.; Mukund, S.; Adams, M. W. W. *J. Am. Chem. Soc.* **1992**, *114*, 3521.

(7) White, H.; Feicht, R.; Huber, C.; Lottspeich, F.; Simon, H. *Biol. Chem. Hoppe-Seyler* **1991**, *372*, 999.

(8) (a) Schmitz, R. A.; Richter, M.; Linder, D.; Thauer, R. K. *Eur. J. Biochem.* **1992**, *207*, 559. (b) Schmitz, R. A.; Albracht, S. P. J.; Thauer, R. K. *Eur. J. Biochem.* **1992**, *209*, 1013.

(9) Deaton, J. C.; Solomon, E. I.; Dunfor, C. N.; Wetherbee, P. J.; Burgess, B. K.; Jacobs, D. B. *Biochem. Biophys. Res. Commun.* **1984**, *121*, 1042.

(10) (a) Personal Communications from Professor D. C. Rees and Professor M. W. W. Adams. (b) Chan, M. K.; Mukund, S.; Kletzin, A.; Adams, M. W. W.; Rees, D. C. *Science* **1995**, *267*, 1463.

(11) Das, S. K.; Biswas, D.; Chaudhury, P. K.; Sarkar, S. *J. Am. Chem. Soc.* **1994**, *116*, 9061.

(12) Eagle, A. A.; Harben, S. M.; Tiekink, E. R. T.; Young, G. C. *J. Am. Chem. Soc.* **1994**, *116*, 9749.

(13) Ueyama, N.; Oku, H.; Nakamura, A. *J. Am. Chem. Soc.* **1992**, *114*, 7310.

(14) (a) Chen, G. *J.-J.*; McDonald, J. W.; Newton, W. E. *Inorg. Chim. Acta* **1976**, *19*, L67. (b) Yu, S.-B.; Holm, R. H. *Inorg. Chem.* **1989**, *28*, 4385. (c) Cervilla, A.; Llopis, E.; Ribera, A.; Domenech, A.; Sinn, E. *J. Chem. Soc., Dalton Trans.* **1994**, 3511.

(15) (a) Harmer, M. A.; Halbert, T. R.; Pan, W. H.; Coyle, C. L.; Cohen, S. A.; Stiefel, E. I. *Polyhedron* **1986**, *5*, 341. (b) Broomhead, J. A.; Enemark, J. H.; Hamner, B.; Ortega, R. B.; Pienkowski, W. *Aust. J. Chem.* **1987**, *40*, 381. (c) Ansari, M. A.; Chandrasekaran, J.; Sarkar, S. *Inorg. Chem.* **1988**, *27*, 763.

(16) (a) Listemann, M. L.; Shrock, R. R.; Dewan, J. C.; Kolodziej, R. M. *Inorg. Chem.* **1988**, *27*, 264. (b) Piepgrass, K.; Pope, M. T. *J. Am. Chem. Soc.* **1989**, *111*, 753.

(17) Sarkar, S.; Das, S. K. *Proc. Indian Acad. Sci.* (*Chem. Sci.*) **1992**, *104*, 533.

(18) Stiefel, E. I.; Bennett, L. E.; Dori, Z.; Crawford, T. H.; Simo, C.; Gray, H. B. *Inorg. Chem.* **1970**, *9*, 281.

parameters were obtained from the measured spectra using DPPH as a calibrant. Conductance measurements were performed at room temperature in MeCN solutions with an Elico CM-82T (Hyderabad, India) conductivity bridge. Cyclic voltammetric measurements were made with CV 27 BAS Bioanalytical Systems. Cyclic voltammograms of 10^{-3} M solutions of the compounds were recorded with glassy carbon working electrode in MeCN containing 0.1 M Et_4NClO_4 as the supporting electrolyte. The experiments employed a Ag/AgCl reference electrode. The values reported are uncorrected for junction potential. Under the same conditions, a ferricenium/ferrocene redox couple was observed at +0.45 V vs Ag/AgCl. All electrochemical experiments were done under a purified dinitrogen atmosphere at 298 K. Gas chromatography experiments were performed with an NUCON GC-5765 using an FID detector/injector (220 °C) and using a SE-30 column (180 °C) with dinitrogen as the carrier gas. The NUCON 5765 program controller was interfaced with a 3300 Series integrator.

Syntheses. $[Bu_4N]_2[W^{VI}O_2(mnt)_2]$. $Na_2WO_4{\cdot}2H_2O$ (0.66 g, 2.0 mmol), Na_2mnt (0.745 g, 4.0 mmol), and $NaHSO_3$ (1.0 g, 9.6 mmol) were dissolved in 80 mL of water, and the pH of reaction mixture was adjusted to 5.5 by adding MeCOOH. $[Bu_4N]Br$ (1.45 g, 4.5 mmol) was added into this solution whereupon an orange solid precipitated. This solid was collected by filtration, washed with 2-propanol and diethyl ether, and crystallized from MeCN solution by adding 2-propanol and diethyl ether: yield 1.16 g (59%); IR (CsI pellet, cm^{-1}) ν(W═O) 916 (vs), 874 (s), ν(W—S) 314 (m), ν(C═C) 1476 (vs), ν(CN) 2198 (vs); UV−vis (MeCN solution, 1×10^{-4} M, nm) 440 (sh), 380; ^{13}C NMR (ppm from TMS) (DMSO-d_6) δ = 123.34, 118.48 (mnt), δ = 57.83, 23.20, 19.26, 13.44 (cation, *n*-Bu_4N); FAB^- (3-nitrobenzyl alcohol) 496 (P^-), 480 (P^- − [O]), 738 (P^- + Bu_4N^+); conductivity (MeCN, 10^{-3} M solution at 298 K) Λ_M = 267 mho cm^2 mol^{-1} (consistent with a 2:1 electrolyte). Anal. Calcd for $C_{49}H_{72}N_6O_2S_4W$: C, 48.96; H, 7.39; N, 8.56; S, 13.07. Found: C, 49.07; H, 7.31; N, 8.63; S, 13.11.

$[Et_4N]_2[W^{VI}O_2(mnt)_2]$ (1). Method 1. $Na_2WO_4{\cdot}2H_2O$ (0.66 g, 2.0 mmol), Na_2mnt (0.745 g, 4.0 mmol), and $NaHSO_3$ (1.0 g, 9.6 mmol) were dissolved in 70 mL of water, and $[Et_4N]Br$ (1.26 g, 6.0 mmol) was then added. The dropwise addition of MeCOOH into the reaction mixture caused the slow precipitation of an orange solid which was kept for 12 h at room temperature for completion. This solid was collected by filtration, washed with cold water, dried, and crystallized from dry MeCN and dry diethyl ether: yield 0.863 g (57%); IR (CsI pellet, cm^{-1}) ν(W═O) 906 (vs), 860 (s), ν(W—S) 310 (m), ν(C═C) 1476 (vs), ν(CN) 2200 (vs); UV−vis (MeCN solution, 1×10^{-4} M, nm) 440 (sh), 380; FAB^- (3-nitrobenzyl alcohol) 496 (P^-), 480 (P^- − [O]), 626 (P^- + Et_4N^+); conductivity (MeCN, 10^{-3} M solution at 298 K) Λ_M = 270 mho cm^2 mol^{-1} (consistent with a 2:1 electrolyte). Anal. Calcd for $C_{24}H_{40}N_6O_2S_4W$: C, 38.09; H, 5.32; N, 11.10; S, 16.94. Found: C, 37.98; H, 5.02; N, 10.94; S, 16.89.

Method 2. $Na_2WO_4{\cdot}2H_2O$ (0.33 g, 1.0 mmol) and oxalic acid $[(COOH)_2{\cdot}2H_2O]$ (0.151 g, 1.2 mmol) were dissolved in 50 mL of water. Na_2mnt (0.373 g, 2.0 mmol) dissolved in 10 mL of water was then added. To the resultant deep orange solution $[Et_4N]Br$ (0.525 g, 2.5 mmol) dissolved in 10 mL of methanol was added to cause the precipitation of the product which was allowed to stand for 6 h for completion. The orange microcrystalline solid was filtered, washed with cold water, and vacuum dried: yield 0.42 g (55%). The IR and UV−vis data were identical to those synthesized by the acetic acid−HSO_3^- method.

$[Ph_4P]_2[W^{VI}O_2(mnt)_2]{\cdot}2H_2O$. $Na_2WO_4{\cdot}2H_2O$ (0.66 g, 2.0 mmol), Na_2mnt (0.745 g, 4.0 mmol), and $NaHSO_3$ (1.0 g, 9.6 mmol) were dissolved in 80 mL of water, and the pH of reaction mixture was adjusted to 5.5 by adding MeCOOH. $[Ph_4P]Br$ (1.68 g, 4.0 mmol) dissolved in a minimum amount of 1:1 methanol−water was then added, whereupon an orange solid precipitated. This solid was filtered, washed with water, and finally extracted in MeCN. Addition of diethyl ether into this MeCN extract followed by keeping for 24 h at 20 °C gave orange red crystals of X-ray diffraction quality: yield 1.40 g (58%) Anal. Calcd for $C_{56}H_{44}N_4O_4P_2S_4W$: C, 55.54; H, 3.66; N, 4.63; S, 10.59. Found: C, 55.20; H, 3.93; N, 4.60; S, 10.28.

$[Et_4N]_2[W^{IV}O(mnt)_2]$ (2). $Na_2WO_4{\cdot}2H_2O$ (0.66 g, 2.0 mmol) and Na_2mnt (0.745 g, 4.0 mmol) were dissolved in 100 mL of deaerated water. The pH of this solution was adjusted to 5.5 by adding MeCOOH. Sodium dithionite (10.0 g, 58.0 mmol) was added, and then addition of $[Et_4N]Br$ (1.26 g, 6.0 mmol) caused slow precipitation of a purple solid. The mixture was allowed to stand at 5 °C for 4 h to complete the precipitation. The solid was collected by filtration and washed with water, 2-propanol, and finally diethyl ether. This purple product was recrystallized from MeCN−diethyl ether as needle-shaped crystals: yield 0.887 g (60%); IR (CsI pellet, cm^{-1}) ν(W═O) 935 (vs), ν(W—S) 325 (w), ν(C═C) 1483 (vs), ν(CN) 2192 (vs); UV−vis (MeCN solution, 1×10^{-4} M, nm) 650, 515, 385 (sh), 355; ^{13}C NMR (ppm from TMS) (DMSO-d_6) δ = 140.42, 118.99 (mnt), 51.53, 7.05 (cation, Et_4N); FAB^- (3-nitrobenzyl alcohol) 480 (P^-), 610 (P^- + Et_4N^+); conductivity (MeCN, 10^{-3} M solution at 298 K) Λ_M = 280 mho cm^2 mol^{-1} (consistent with 2:1 electrolyte). Anal. Calcd for $C_{24}H_{40}N_6OS_4W$: C, 38.91; H, 5.44; N, 11.34; S, 17.31. Found: C, 38.88; H, 5.56; N, 11.44; S, 17.40.

Synthesis of 2 from $[Et_4N_2]_2[W^{VI}O_2(mnt)_2]$ (1) and H_2S/Ph_3P. Into H_2S-saturated CH_2Cl_2(10 mL) were added $[Et_4N]_2[W^{VI}O_2(mnt)_2]$ (0.19 g, 0.25 mmol) and Ph_3P (0.132 g, 0.5 mmol), and the solution was allowed to stand for 48 h at room temperature when the orange red solution turned to purple. The solution was evaporated under vacuum, the residue was dissolved in 8.0 mL of MeCN, and excess of diethyl ether was added. Upon standing overnight in the refrigeration the precipitated microcrystalline solid was filtered and washed with diethyl ether. This solid was spectrally identified as **2**: yield 0.17 g (92%).

$[Et_4N]_2[W^{VI}O(S_2)(mnt)_2]$ (3). The complex $[Et_4N]_2[W^{IV}O(mnt)_2]$ (**2**) (0.74 g, 1.00 mmol) and elemental sulfur (0.08 g, 2.49 matom) were taken in acetone (60 mL) and refluxed under argon for 36 h whereby the purple color of **2** turned red. The red solution was evaporated under vacuum to an oily mass and was extracted with MeOH (15 mL). Addition of diethyl ether into the extract and standing overnight at 20 °C resulted in the isolation of **3** as deep red crystals: yield 0.42 g (52%); mp 124−126 °C dec; IR (CsI pellet, cm^{-1}) ν(W═O) 920 (s), ν(S—S) 532 (m), ν(C═C) 1470 (s), ν(CN) 2197 (s); UV−vis (MeCN solution, 1×10^{-4} M, nm) 478, 385; ^{13}C NMR (ppm from TMS) (DMSO-d_6) δ 128.2, 128.0, 120.2, 119.1, 118.9, 117.4, 116.6 (mnt), 51.6, 7.1 (cation, Et_4N); ^{1}H NMR (ppm from TMS) (CD_3CN) δ = 3.6 (q, cation CH_2), 1.7 (t, cation CH_3); FAB^- (3-nitrobenzyl alcohol) 544 (P^-) 512 (P^- − [S]), 480 (P^- − 2[S]), 674 (P^- + Et_4N^+); conductivity (MeCN, 10^{-3} M solution at 298 K) Λ_M = 300 mho cm^2 mol^{-1} (consistent with a 2:1 electrolyte). Anal. Calcd for $C_{24}H_{40}N_6OS_6W$: C, 35.81; H, 5.01; N, 10.44; S, 23.90. Found: C, 35.83; H, 4.90; N, 10.57; S, 23.85.

Attempted Synthesis of $[W^{VI}OS(mnt)_2]^{2-}$: (a) Using $WO_2S_2^{2-}$ and WOS_3^{2-}. (i) $(NH_4)_2WO_2S_2$ (0.632 g, 2.0 mmol) and Na_2mnt (0.745 g, 4.0 mmol) were dissolved in 100 mL of water. $[Et_4N]Br$ (1.26 g, 6.0 mmol) was added, and the pH of the solution was adjusted to 5.5 by adding MeCOOH whereby the yellow color of the solution turned deep reddish brown. On standing overnight a red brown solid precipitated out from the solution. This was filtered, washed with water, and dried under vacuum. The crude product was treated with methanol wherein a portion of the solid dissolved. This was filtered, the residue was washed with methanol, and the methanol extract with washings was concentrated. Addition of diethyl ether and standing overnight at 20 °C yielded deep red crystals which on spectroscopic analysis was found to be **3**: yield 0.483 g (30%). The methanol insoluble purple color residue was recrystallized from MeCN−diethyl ether and characterized as **2**: yield 0.148 g (10%).

(ii) A similar procedure was adopted using $(NH_4)_2WOS_3$ (0.664 g) instead of $(NH_4)_2WO_2S_2$ wherein the compound isolated was predominantly **3**, yield of 0.741 g (50%) with the formation of **2** as the minor product (0.076 g, 5%).

(b) Using Na_2WO_4 and H_2S. $Na_2WO_4{\cdot}2H_2O$ (0.33 g, 1.0 mmol) was dissolved in 50 mL of water, and H_2S was bubbled through this solution for 5 min to develop a pale yellow color. Oxalic acid (0.151 g, 1.2 mmol) was added into it whereby the color of the solution deepened. Na_2mnt (0.372 g, 2.0 mmol) dissolved in 20 mL of methanol was added, resulting in the color change of the solution to deep red. $[Et_4N]Br$ (0.63 g, 3.0 mmol) dissolved in 20 mL of water was added, and passage of H_2S was stopped. Upon standing overnight at 20 °C, a deep red compound separated out. This was filtered, washed with water, and dried under vacuum. This solid was found to be a mixture of compounds under the microscope. Elemental sulfur impurity was removed by benzene washing. The remaining solid in MeCN showed the presence of **2** and **3** by electronic spectroscopy. **2** and **3** were

Table 1. Experimental Details of the X-ray Diffraction Studies

	$[Ph_4P]_2[W^{VI}O_2(mnt)_2]\cdot 2H_2O$ (**1**)	$[Et_4N]_2[W^{IV}O(mnt)_2]$ (**2**)	$[Et_4N]_2[W^{VI}O(S_2)(mnt)_2]$ (**3**)
crystal size, mm	0.4 × 0.2 × 0.15	0.6 × 0.3 × 0.1	0.4 × 0.4 × 0.3
chem form	$C_{56}H_{44}N_4O_4P_2S_4W$	$C_{24}H_{40}N_6OS_4W$	$C_{24}H_{40}N_6OS_6W$
fw	1211.03	740.71	804.83
cryst syst	orthorhombic	orthorhombic	monoclinic
space group	*Pbcn*	$P2_12_12$	$P2_1/a$
a, Å	20.526(3)	14.78(3)	12.238(3)
b, Å	15.791(3)	30.08(2)	18.873(2)
c, Å	17.641(3)	7.37(4)	15.026(2)
β, deg			102.84(2)
Z	4	4	4
V, Å^3	5713.9(2.1)	3276.6(1.9)	3383.7(1.4)
d_{calcd}, gm cm^{-3}	1.365	1.502	1.517
μ(Mo Kα), cm^{-1}	22.6	38.1	37.5
no. of data colltd	5012	3900	6256
no. of data used ($F_o > 3\sigma(F_o)$)	3386	3541	4962
R	0.044	0.064	0.036
R_w	0.042	0.052	0.033
largest shift/esd final	0.002	0.002	0.002
largest peak, e/Å^3	0.50	0.42	0.46
no. of params	333	333	342

separated as described earlier. However, variations in the time for the passage of H_2S did not result in the isolation of either **2** or **3** as the single product.

(c) Using $[Et_4N]_2[W^{VI}O_2(mnt)_2]$ and H_2S. A methanolic solution (20 mL) of $[Et_4N]_2[W^{VI}O_2(mnt)_2]$ (0.38 g, 0.5 mmol) was saturated with H_2S by passing it for 15 min. Addition of excess diethyl ether and standing overnight in the refrigerator yielded mostly the starting material contaminated with a small quantity of **2** and traces of elemental sulfur. However, after the passage of H_2S when the solution was heated to 50 °C for about 2 h, the color of the solution turned purplish red. Reduction of the volume of the solution to 10 mL followed by the addition of 25 mL of 2-propanol and standing in refrigerator led to the isolation of pure **2** in 55% yield. On further standing, the mother liquor after the addition of excess of 2-propanol yielded another crop of **2** mixed with red crystals of **3**.

Reaction of 2 with Na_2MoO_4: Synthesis of $[Et_4N]_2[Mo^{IV}O(mnt)_2]$ by an Intermetallic Electron Transfer Reaction. **2** (0.192 g, 0.26 mmol) dissolved in 10 mL of MeCN was added into a stirred solution of sodium molybdate (0.125 g, 0.52 mmol) in water (8 mL of acetate buffer, pH 4.65). Stirring was continued for 24 h whereupon the purple color changed to yellow green. Water (10 mL) was added, and on standing for 2 days at room temperature, needle-shaped crystals of $[Et_4N]_2[Mo^{IV}O(mnt)_2]$ separated out: yield 0.110 g (65%). Anal. Calcd for $C_{24}H_{40}MoN_6OS_4$: C, 44.15; H, 6.17; N, 12.87; S, 19.64. Found: C, 44.09; H, 6.29; N, 12.79; S, 19.61. The spectral features and cyclic voltammogram of this complex matched exactly with those reported for $[Et_4N]_2[Mo^{IV}O(mnt)_2]$.[11]

Reaction of 3 with Ph_3P: Synthesis of $[Et_4N]_2[W^{IV}O(mnt)_2]$ by Sulfur Atom Transfer Reaction. Ph_3P (0.042 g, 0.158 mmol) dissolved in 5 mL of MeCN was added to a solution of complex **3** (0.064 g, 0.079 mmol) in 5 mL of MeCN. This was stirred for 4 h when the red color of the solution changed to purple. Addition of excess diethyl ether resulted in the isolation of needle-shaped purple crystals whose spectroscopic properties were identical to those of **2**. The yield of **2** was 0.049 g (83%). The combined filtrate with washings were evaporated to dryness and extracted with diethyl ether, which yielded Ph_3PS: 0.045 g (98%); mp 272 °C; mass $m/z = 294$.

Reaction of 2 under Acidic Condition Using 1 Equiv of Na_2mnt: Synthesis of $[Et_4N]_2[W^{IV}(mnt)_3]$. **2** (0.150 g, 0.203 mmol) dissolved in 10 mL of MeCN was added into an aqueous solution (10 mL) of Na_2mnt (0.030 g, 0.161 mmol) with stirring. Trichloroacetic acid dissolved in water was added dropwise into the reaction mixture to adjust the pH of the solution to 2.0. After being stirred for 1 h, the deep red-violet solution was diluted with an excess of water, causing precipitation of a microcrystalline solid of $[Et_4N]_2[W^{IV}(mnt)_3]$: yield 0.159 g (91%). Anal. Calcd for $C_{28}H_{40}WN_8S_6$: C, 38.88; H, 4.66; N, 12.95; S, 22.24. Found: C, 39.14; H, 4.86; N, 13.02; S, 22.12. The spectral and electrochemical data of this complex matched exactly with those of the reported $[W^{IV}(mnt)_3]^{2-}$.[19]

Reaction of 2 under Similar Acidic Condition without Na_2mnt. Similar acidification by trichloroacetic acid and subsequent operations as described above led to the isolation of $[Et_4N]_2[W^{IV}(mnt)_3]$, which was recrystallized from MeCN−H_2O to yield 0.10 g (57%) of the pure complex displaying identical spectroscopic properties of the authentic tris-dithiolene compound.[19]

X-ray Structure and Determination. Diffraction quality air-stable orange red crystals of $[Ph_4P]_2[W^{VI}O_2(mnt)_2]\cdot 2H_2O$ were obtained directly by synthetic purification method. Needle-shaped purple crystals of $[Et_4N]_2[W^{IV}O(mnt)_2]$ (**2**) were grown from MeCN solution by layering it with diethyl ether at 10 °C and allowing it to stand overnight. Red cubic crystals of $[Et_4N]_2[W^{VI}O(S_2)(mnt)_2]$ (**3**) were obtained on standing the solution in MeOH−diethyl ether at 10 °C for 24 h. A single crystal for each complex was sealed in a glass capillary under argon atmosphere for the X-ray measurements. X-ray measurements were performed at 25 °C on a Enraf-Nonius CAD4 diffractometer equipped with a Mo X-ray source and a graphite monochromator.

Intensity data for all crystals were obtained with the use of a $\theta-2\theta$ step scan technique. For each data set collected, three standard reflections were monitored (periodically) after every 97 reflections and showed no significant decay during the data collection. Lattice parameters were obtained from a least-squares analysis of 25 machine-centered reflections with $20° < 2\theta < 30°$. The basic crystallographic parameters for $[Ph_4P]_2[W^{VI}O_2(mnt)_2]\cdot 2H_2O$, **2**, and **3** are listed in Table 1. The data were corrected for Lorentz and polarization effects, and absorption corrections were applied.

The structures were solved by the direct method using the XTAL 3.2 package.[20] The structures were refined by full-matrix least-squares methods. All non-hydrogen atoms of each of the crystals were refined anisotropically. All hydrogen atoms were placed on the calculated positions with a assumed C−H distance of 0.95 Å. Compound **2** crystallizes in the acentric space group $P2_12_12$. Anomalous dispersion corrections were applied, and we have checked for the correct enantiomer. The coordinates of the atoms given belong to the correct enantiomer. A PC-486 computer was used for all calculations. Details of the structure determination are given in the supporting information as are complete tables of positional and thermal parameters, calculated hydrogen atom positions, bond distances and angles, and calculated and observed structure factors.

Kinetic Measurements of the Sulfur Atom Transfer Reaction between 3 and Ph_3P. All kinetic measurements were carried out by the spectrophotometric method by the use of a Shimadzu 160 spectrophotometer provided with a piezoelectric-type thermostating device for the regulation of temperature. A stock solution of the complex **3** in MeCN of fixed concentration (2.00×10^{-4} M) and a stock solution of Ph_3P in MeCN of fixed concentration (7.28×10^{-4}

(19) McCleverty, J. A.; Locke, J.; Wharton, E. J. *J. Chem. Soc. A* **1968**, 816.

(20) *XTAL3.2 Reference Manual*; Hall, S. R., Flack, H. D., Stewart, J. M., Eds.; University of Western Australia: Geneva and Maryland, 1992.

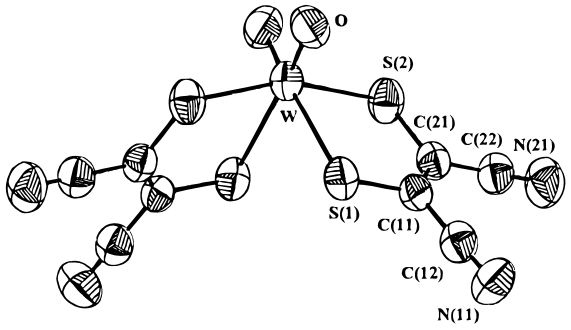

Figure 1. Structure and labeling of the $[W^{VI}O_2(mnt)_2]^{2-}$ anion in $[Ph_4P]_2[W^{VI}O_2(mnt)_2]\cdot 2H_2O$. Thermal ellipsoids as drawn by ORTEP represent the 50% probability surfaces.

Table 2. Selected Bond Distances (Å) and Angles (deg) in $[W^{VI}O_2(mnt)_2]^{2-}$

	Bond Distances		
W═O	1.701(6)	S(1)−C(11)	1.723(8)
W−S(1)	2.622(3)	S(2)−C(22)	1.730(8)
W−S(2)	2.445(2)	C(11)−C(21)	1.35(1)
	Bond Angles		
S(1)−W−O	164.5(3)	S(2)−C(21)−C(11)	124.3(6)
S(2)−W−O	85.6(2)	S(2)−C(21)−C(22)	115.3(6)
W−S(2)−C(21)	108.0(3)	N(21)−C(22)−C(21)	178.5(9)

M) were made. In a typical experiment, a cell (path length 1 cm) containing the solution of **3** (1.5 mL) was fitted with a serum cap and placed in the thermostated cell compartment. After thermal equilibration, 1.5 mL of Ph_3P solution was withdrawn from the stock solution which was thermally preequilibrated at the same temperature and was injected through the serum cap and the cell contents were quickly mixed by shaking. Then the progress of the reaction was monitored by the decay of absorbance (478 nm) as a function of time. The rate law was found to be second order:

$$\frac{d[W(VI)]}{dt} = -k_2[W(VI)][Ph_3P]$$

The decay of the complex **3** in terms of concentration follows eq 2,

$$c_t = (A_t - A_\alpha)/(\epsilon_1 - \epsilon_2) \qquad (2)$$

where c_t is the molar concentration of the complex **3** at the time t and A_t and A_α are the absorbances of the reaction mixture solution at time t and at time $t = \alpha$, respectively. ϵ_1 and ϵ_2 are the molar extinction coefficients of complexes **3** and **2**, respectively, at 478 nm in MeCN.

The observed rate constants (k_2) were obtained from the second-order decay curves for the progress of each reaction completing at least three half-lives. Three kinetic runs were made for each reaction. All computations for data analysis were performed with locally written programs on a Hewlett-Packard (HP 9000) computer.

Results and Discussion

Description of Structures. (a) $[Ph_4P]_2[W^{VI}O_2(mnt)_2]\cdot 2H_2O$. For $[Ph_4P]_2[W^{VI}O_2(mnt)_2\cdot 2H_2O$ in the space group *Pbcn*, the molecule has a 2-fold symmetry, the W atom lies on the crystallographic 2-fold symmetry, and only one-half of the molecule is present in the asymmetric unit. The oxygen atom of one of the water molecules is also situated on a crystallographic 2-fold axis. The structure of the anion, $[W^{VI}O_2(mnt)_2]^{2-}$, is shown in Figure 1, and selected bond distances and angles are listed in Table 2. The W═O distance (1.701(6) Å) is shorter than the W═O distances (1.727(9) Å and 1.737(6) Å] reported for $[Ph_4P]_2[W^{VI}O_2(bdt)_2]$.[13] The W−S distance (2.622(3) Å) *trans* to W═O and the W−S distance (2.445(2) Å) *cis* to W═O are longer than those of corresponding molybdenum complexes.[11] For $[Ph_4P]_2[W^{VI}O_2(bdt)_2]$, the mean W−S distance (2.597(4) Å) *trans* to W═O and the mean W−S distance (2.425(4) Å) *cis* to W═O[13] are shorter than those of $[Ph_4P]_2[W^{VI}O_2(mnt)_2]\cdot 2H_2O$ but similar to those of $[Mo^{VI}O_2(mnt)_2]^{2-}$.[11] The intraligand distances and angles are unexceptional.

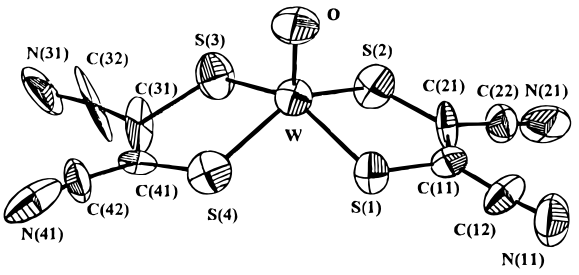

Figure 2. Structure and labeling of the $[W^{IV}O(mnt)_2]^{2-}$ anion in $[Et_4N]_2[W^{IV}O(mnt)_2]$. Thermal ellipsoids as drawn by ORTEP represent the 50% probability surfaces.

Table 3. Bond Distances (Å) and Selected Angles (deg) in $[W^{IV}O(mnt)_2]^{2-}$

	Bond Distances		
W═O	1.73(2)		
W−S(1)	2.368(9)	W−S(4)	2.362(7)
W−S(2)	2.392(7)	W−S(3)	2.37(1)
S(1)−C(11)	1.87(3)	S(3)−C(31)	1.88(3)
S(2)−C(21)	1.73(3)	S(4)−C(41)	1.66(3)
C(11)−C(21)	1.35(5)	C(31)−C(41)	1.26(6)
C(11)−C(12)	1.38(5)	C(31)−C(32)	1.36(8)
C(21)−C(22)	1.32(3)	C(41)−C(42)	1.28(3)
N(11)−C(12)	1.20(5)	N(31)−C(32)	1.27(8)
N(21)−C(22)	1.08(3)	N(41)−C(42)	1.02(4)
	Bond Angles		
S(1)−W−S(2)	84.1(3)	S(3)−W−S(4)	83.3(3)
S(1)−W−S(3)	147.7(2)	S(1)−W−O	107.1(9)
S(1)−W−S(4)	86.6(3)	S(2)−W−O	108.0(6)
S(2)−W−S(3)	84.5(3)	S(3)−W−O	105.1(9)
S(2)−W−S(4)	140.7(2)	S(4)−W−O	111.2(6)

(b) $[Et_4N]_2[W^{IV}O(mnt)_2)]$ (2). In **2**, One Et_4N^+ cation is in a general position and the two cations (N(6) and N(7)) are in special positions. The structure of the $[W^{IV}O(mnt)_2]^{2-}$ anion is shown in Figure 2. Selected structural parameters are shown in Table 3. The W(IV) ion is square-pyramidally coordinated by two mnt^{2-} ligands which occupy the equatorial positions of the distorted square pyramid. The terminal axial oxo ligand with a W^{IV}═O bond (1.73(2) Å) is similar in length with that in $[W^{IV}O(bdt)_2]^{2-}$.[13] The unequal W−S bonds in **2** have a mean value (2.378(5) Å) similar to the corresponding value (2.372(4) Å) for $[W^{IV}O(bdt)_2]^{2-}$.[13] An examination of the rectangle of sulfur donors in the equatorial plane of **2** shows that the S(1)−S(2) intraligand distance (3.19(1) Å) is very close to the S(2)−S(3) interligand contact (3.20(1) Å) whereas the S(3)−S(4) intraligand distance (3.14(1) Å) is the closest and the S(1)−S(4) interligand contact (3.245(9) Å) is the longest. The inequalities in O−W−S angles and in W−S bonds contribute to the differences in S···S interactions. The other distances and angles are unexceptional.

(c) $[Et_4N]_2[W^{VI}O(S_2)(mnt)_2]$ (3). Figure 3 shows the seven-coordinated structure of the $[W^{VI}O(S_2)(mnt)_2]^{2-}$ anion. Selected bond distances and angles are listed in Table 4. The S(5)−S(6) distance in the disulfur group is 2.032(3) Å, which is comparable with 2.043(2) Å in $[WO(S_2)(S_2CNEt_2)_2]$.[15b] The W═O bond (1.689(4) Å) is shorter than that (1.706(3) Å) reported for $[WO(S_2)(S_2CNEt_2)_2]$.[15b] An examination of the W−S bonds show that the W−S(5) and W−S(6) bonds of the disulfido group (2.389(2) and 2.420(2) Å, respectively) are shortest and the W−S(4) bond (of the dithiolene sulfur) (2.615(2) Å) *trans* to the terminal oxo group is longest. An examination of the deformed pentagon of sulfur donors in the

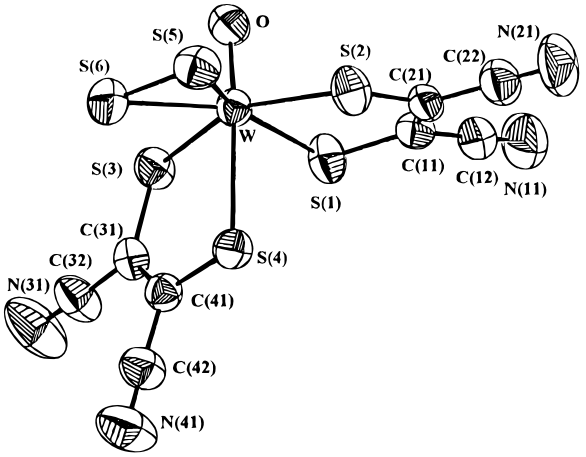

Figure 3. Structure and labeling of the $[W^{VI}O(S_2)(mnt)_2]^{2-}$ anion in $[Et_4N]_2[W^{VI}O(S_2)(mnt)_2]$. Thermal ellipsoids as drawn by ORTEP represent the 50% probability surfaces.

Table 4. Selected Bond Distances (Å) and Angles (deg) in $[W^{VI}O(S_2)(mnt)_2]^{2-}$

	Bond Distances		
W═O	1.689(4)	S(5)−S(6)	2.032(3)
W−S(1)	2.509(2)	W−S(4)	2.615(2)
W−S(2)	2.438(2)	W−S(5)	2.389(2)
W−S(3)	2.508(2)	W−S(6)	2.420(2)
	Bond Angles		
O−W−S(1)	90.6(2)	S(1)−W−S(2)	80.61(6)
O−W−S(2)	101.6(2)	S(1)−W−S(3)	74.37(6)
O−W−S(3)	88.3(2)	S(2)−W−S(5)	73.44(6)
O−W−S(5)	100.8(1)	S(3)−W−S(6)	79.84(7)
O−W−S(6)	96.9(2)	S(5)−W−S(6)	49.97(7)

equatorial plane of **3** shows short S(1)−S(3) and long S(2)−S(3) interligand contacts (3.031(4) and 4.812(3) Å, respectively) compared to S(1)−S(2) and S(3)−S(4) intraligand contacts (3.202(3) and 3.299(5) Å, respectively). Bond lengths and angles within the mnt^{2-} ligands of **3** are similar to the corresponding values found for $[Ph_4P]_2[W^{VI}O_2(mnt)_2]\cdot 2H_2O$ and **2** and for $[Mo^{VI}O_2(mnt)_2]^{2-}$.[11] The WOS_6 core structure of **3** is consistent with that of $[WO(S_2)(S_2CNEt_2)_2]$.[15b]

Synthesis. WO_4^{2-} in neutral aqueous medium does not react with Na_2mnt. The reported reaction to isolate $[W^{IV}(mnt)_3]^{2-}$ involved the reaction between WCl_6 or WO_2Cl_2 and Na_2mnt in alcoholic medium.[19] Chloro compounds of tungsten(VI) on alcoholysis produce hydrochloric acid, and so this reaction is mainly carried out in strongly acidic medium. We have observed that pure $[Et_4N]_2[W^{VI}O_2(mnt)_2]$ (**1**) did produce $[Et_4N]_2[W^{IV}(mnt)_3]$ on acidification in methanol. Protonation of oxo groups on acidification and subsequent reduction of W(VI) by dithiolene could be related to the nonavailability of sufficient mnt^{2-}, resulting in the low yield of $[W^{IV}(mnt)_3]^{2-}$. For aqueous WO_4^{2-}, when the pH is lowered from 7, expansion of the coordination number of WO_4^{2-} is effected by polyoxoanion formation. The evidence for the presence of a WO_2^{2+} moiety in equilibrium with these polyanions is lacking.[21] To avoid any degree of oxidation of mnt^{2-} by polytungstate anions around pH 5.5 (acetate buffer), we have carried out the reaction between Na_2WO_4 and Na_2mnt in aqueous medium in the presence of an excess of HSO_3^-. Addition of countercation (Et_4N^+/Bu_4N^+) drives the reaction in the desired way by phasing out the complex salt of **1** from the reaction medium. Replacement of HSO_3^- by excess of $S_2O_4^{2-}$ in this synthetic procedure resulted in the isolation of **2** in 60% yield. Interestingly, $S_2O_4^{2-}$ is used as the "universal" *in vitro* reductant for all the reported molybdoenzymes including nitrogenase and for thermophilic tungstoenzymes. Early studies to synthesize $WO(R_2dtc)_2$ analogous to $MoO(R_2dtc)_2$[22] using dithionite led to the isolation of pentavalent dimeric species.[23] This might be due to the fact that, when R_2dtc^- and WO_4^{2-} were present together and dithionite was added in a slightly acidified condition, the reduction of tungsten(VI) to tungsten (IV) was not fully achieved, which resulted in the formation of the $\{W_2^VO_3\}$ core as $[W^{VI}O_2(R_2dtc)_2] + [W^{IV}O(R_2dtc)_2] \rightarrow [W_2^VO_3(R_2dtc)_4]$. In the present case, this comproportionation reaction does not take place and the appreciable solubility of the $[Et_4N]^+$ salt of the W(VI) complex led to its slow reduction (by dithionite) to the W(IV) complex which, being insoluble in the reaction medium, is precipitated out.

The instability of **2** at pH < 4 led to the isolation of $[W^{IV}(mnt)_3]^{2-}$ in 57% yield which is increased to over 90% yield in the presence of 1 equiv of Na_2mnt, suggesting reaction 3.

$$[(mnt)_2W^{IV}{=}O]^{2-} + H_2O(H^+) \longrightarrow$$

$$\{(mnt)_2W^{IV}(OH)_2\}^{2-} \longrightarrow {}^2/_3[W^{IV}(mnt)_3]^{2-} + {}^1/_3W^{IV}$$

$$\downarrow\ mnt^{2-},\ 2H^+$$

$$[W^{IV}(mnt)_3]^{2-} + 2H_2O \qquad (3)$$

The reaction between **2** and MoO_4^{2-} in aqueous acetonitrile medium (pH ∼ 5.0, acetate buffer) results in the isolation of $[Mo^{IV}O(mnt)_2]^{2-}$ in 65% yield. Treatment of **2** with elemental sulfur in refluxing acetone resulted in the oxidative addition reaction with the formation of **3**. Attempted synthesis of $[W^{VI}OS(mnt)_2]^{2-}$ from the reaction of $[W^{VI}O_2S_2]^{2-}$ (or $[W^{VI}OS_3]^{2-}$) with mnt^{2-} always results in the isolation of a mixture of **2** and **3** (*vide supra*). This suggests the possible involvement of intramolecular redox reaction across tungsten−sulfur bond of the unstable $[W^{VI}OS(mnt)_2]^{2-}$ species with the initial formation of **2** and elemental sulfur, and finally a mixture of **2** and **3** is obtained. These reactions are important in understanding the incorporation of tungsten into molybdopterin in the biosynthesis of AOR enzyme under sulfiding conditions. Regeneration of **2** by the reaction of **3** with Ph_3P with the formation of Ph_3PS is an example of a sulfur atom transfer reaction. In all of these and subsequent reactions to be discussed, the participation of biologically irrelevant $W_2(V)$ dimer did not take place. This is now a common feature of all anionic bis-dithiolene monooxo- and dioxomolybdenum and -tungsten complexes reported to date.[11,13]

Effective Potentials in Atom Transfer Reactions with Biological Perspectives. Complexes **1** and **3** showed irreversible reduction with reduction peak potentials at −1.50 and −1.45 V (vs Ag/AgCl in MeCN), respectively. The reduction peak potential of **1** apparently did not shift lower to −1.50 V when carried out in MeCN containing acetic acid−water (3.5 M water) at pH 5.5 (At −1.3 V, a reduction process associated with the reduction of proton appeared). Sodium dithionite has an effective reduction potential of −0.775 V vs Ag/AgCl at pH 5.5.[24] Thus, on the basis of simple reduction potential values, dithionite should not be able to reduce **1**. Contrary to this, dithionite smoothly reduced **1** to **2**. The progress of this reaction was monitored spectrophotometrically by following the appear-

(21) Pope, M. T.; Still, E. R.; Williams, R. J. P. In *Molybdenum and* Molybdenum *Containing Enzymes*; Coughlan, M. P., Ed.; Pergamon Press: Oxford, U. K., 1980; p 1.

(22) Jowitt, R. N.; Mitchell, P. C. H. *J. Chem. Soc.* **1969**, 1476.

(23) Lozano, R.; Alarcon, E.; Doadrio, A. L.; Doadrio, A. *Polyhedron* **1983**, *2*, 435.

(24) This value is a rough estimate of upper limit as E_o' of dithionite varies with concentration, see: Lambath, D. O.; Palmer, G. *J. Biol. Chem.* **1973**, *248*, 6095. For pH effect, see: Mayhow, S. G. *Eur. J. Biochem.* **1978**, *85*, 535.

ance of two characteristic absorption bands at 515 and 650 nm for **2** with a clean isosbestic point at 600 nm (see supporting information). This smooth reduction of **1** to **2** by dithionite demonstates that this reaction must involve an inner sphere mechanism.[25] Most of the oxomolybdo- and tungstoenzymes are involved in atom transfer reactions. The active site of the enzyme (E) and the substrate (S) first form the Michaelis complex, ES, wherein the chemical identity of free E and unbound S are lost. The unstable ES complex can spontaneously engage in intramolecular electron transfer followed by or coupled to an atom transfer reaction with the desorption of the oxidized substrate from the reduced E for an oxidase type half-reaction. This reaction process cautions that the cause of atom transfer reactions may not be predictable from using only the electron transfer concept[26] and reduction potential values measured by cyclic voltammetry for model compounds or by spectroscopy coupled to potentiometry using mediator dye for native enzymes. Thus, for the Mo(VI)/Mo(V) and Mo(V)/Mo(IV) couples of dimethyl sulfoxide (DMSO) reductase, the measured midpoint potential values range between +0.065 and −0.15 V *vs* NHE in the pH range 5−9[27]. However, DMSO, the substrate for this enzyme, is electrochemically stable over a large range of potentials from far positive to far negative values and, in fact, is used as a solvent for electrochemical studies. For the complexes, $[Mo^{IV}O(Et_2dtc)_2]$ and $[Mo^{IV}O(LNS)_2DMF]$ (dtc = dithiocarbamate; $LN(SH)_2$ = 2,6-bis(2,2-diphenyl-2-mercaptoethyl)pyridine), the difference of 0.12 V in the appearance of irreversible anodic peak potentials (+0.4[28] and +0.52 V[29] vs SCE respectively) did not distinguish their thermodynamic ability to reduce DMSO. Hence the difference of only −0.03 V for the Mo(V)/Mo(IV) couples between the oxosulfido (active) and dioxo (inactive) forms of bovine xanthine oxidase[30] should not be fully responsible for the difference in their activity on xanthine. These observations clearly suggest the inherent chemistry associated with a species to form the enzyme−substrate complex. The possible existence of such a species in the reductive half-reaction of xanthine oxidase has recently been reported.[31]

1 with PhSH (reduction potential, +0.6 V and for PhS^- = −0.31 V vs $Ag/AgNO_3$ (MeCN)[32]) or DTT (1,4-dithiothreitol, reduction potential, −0.33 V vs NHE)[33] slowly reacts to yield **2** and the reaction possibly follows the course as shown in equation 4. The slow conversion of **2** (40% conversion was

$$[W^{VI}O_2(mnt)_2]^{2-} \xrightarrow{PhSH} [W^{VI}O(OH)(SPh)(mnt)_2]^{2-} \xrightarrow{PhSH} [W^{VI}O(SPh)_2(mnt)_2]^{2-} \rightarrow [W^{IV}O(mnt)_2]^{2-} + PhSSPh + H_2O \quad (4)$$

measured spectrophotometrically at a temperature of 30 °C after 12 h in MeCN, and the byproduct PhSSPh has been identified by its elemental analysis and melting point) has been monitored by EPR spectroscopy, and the reaction mixture remained EPR silent during the entire course of the reaction. Thus, the stepwise one-electron redox reaction with the involvement of the $PhS^{\bullet}$ radical and W(V) center is unlikely.[34] This suggests the formation of $[W^{VI}O(SPh)_2(mnt)_2]^{2-}$ (eq 4), which responded to disulfide elimination with the concomitant reduction of tungsten(VI) by two oxidation states.[35] Interestingly, the reaction of **1** with H_2S saturated in CH_2Cl_2, MeCN, or MeOH did not lead to any apparent substitution of the oxo group by the sulfido group, but on prolong standing at room temperature (5 days), **1** changed predominantly to **3** as observed spectrophotometrically. Under H_2S, quick phasing out of the complex by diethyl ether resulted in the isolation of unreacted **1** with a trace amount of **2** and elemental sulfur. Warming the solution for a couple of hours led to the conversion of **1** to **2** in moderate yield along with the formation of **3** (*vide supra*). Ph_3P alone very slowly reacts with **1** in CH_2Cl_2 to form **2** (15% conversion after 48 h) with the formation of Ph_3PO. However, in the presence of Ph_3P, **1** with saturated H_2S in CH_2Cl_2 was completely reduced to **2** within 48 h with the formation of Ph_3PS (*vide supra*). Hence the reaction between **1** and H_2S/Ph_3P presumably follows the same path as under H_2S alone. Here the formation of **3** is prevented by the depletion of elemental sulfur which is used up in the formation of Ph_3PS with Ph_3P catalyzed by **2** (*vide infra*). In all these reactions described here using H_2S, we failed to observe any species containing the $\{W^{VI}OS\}$ moiety, which, if formed at all, should be very susceptible to an intramolecular electron transfer reaction across the W═S bond.

The reaction of **3** with thiophiles is similar to that of the $[MoO(S_2)(R_2dtc)_2]$ complex.[36] With PhSH it yielded **2** with the production of H_2S and PhSSPh. Contrary to the molybdenum compound, no dimeric W(V) compound is formed. However, with Ph_3P or CN^-, a single step reaction (eq 5) occurred as represented below:

$$[W^{VI}O(S_2)(mnt)_2]^{2-} + 2Ph_3P \rightarrow [W^{IV}O(mnt)_2]^{2-} + 2Ph_3PS \quad (5)$$

The progress of this reaction, as observed spectrophotometrically, showed a clean isosbestic point at 365 nm (see the supporting information). Addition of 1 equiv of Ph_3P led to a 0.5 equiv conversion of **3** to **2**, and the resultant electronic spectrum was a superposition of the electronic spectra of **3** and **2**, each taken in a 0.5 equiv amount. Similar conversion using $[MoO(S_2)(Et_2dtc)_2]$ has been reported.[36]

Kinetics of Reaction 5. The kinetics of the forward reaction between **3** and Ph_3P (eq 5) were followed by monitoring the decay of the 478 nm absorption band at **3** in MeCN. This reaction followed second-order (A + 2B type) kinetics with an observed rate constant of $k_2 = 4.3$ (± 0.06) M^{-1} s^{-1} in MeCN at 25 °C. Activation parameters were obtained by a least-squares fit of k_2 values measured at different temperatures to the Eyring eq 6, as shown in Figure 4.

$$k_2 = (K_B T/h) \exp[(\Delta S^{\ddagger}/R) - (\Delta H^{\ddagger}/RT)] \quad (6)$$

Rate constants at different temperatures and activation parameters for reaction 5 are presented in Table 5. For a side-on bound S_2^{2-} ligand, it is known that a cycloaddition of an alkyne to a metal side-on bound S_2^{2-} could be a symmetry-forbidden process.[37] Thus the reaction between $[Mo_2S_6O_2]^{2-}$ and the activated acetylene DMAC (dimethylacetylenedicarboxylic acid)

(25) (a) Anbar, M.; Taube, H. *J. Am. Chem. Soc.* **1958**, *80*, 1073. (b) Sfritar, J. A.; Taube, H. *J. Am. Chem. Soc.* **1969**, *8*, 2281.
(26) Bennett, L. E. *Prog. Inorg. Chem.* **1973**, *18*, 1.
(27) Weiner, J. H.; Cammack, R. *Biochemistry* **1990**, *29*, 8410.
(28) DeHayes, L. J.; Faulkner, H. C.; Doub, W. H., Jr.; Sawyer, D. T. *Inorg. Chem.* **1975**, *14*, 2110.
(29) Berg, J. M.; Holm, R. H. *J. Am. Chem. Soc.* **1985**, *107*, 917.
(30) (a) Barber, M. J.; Siegal, L. M. *Biochemistry* **1982**, *21*, 1638. (b) Pilato, R. S.; Stiefel, E. I. In *Bioinorganic Catalysis*; Reedijk, J., Ed.; Marcell Dekker, Inc: New York, 1993; p 131.
(31) Mondal, M. S.; Mitra, S. *Biochemistry* **1994**, *33*, 10305.
(32) Bradbury, J. R.; Masters, A. F.; McDonell, A. C.; Brunette, A. A.; Bond, A. M.; Wedd, A. G. *J. Am. Chem. Soc.* **1981**, *103*, 1959.
(33) In *Merck Index*, 9th ed.; Merck & Co., Inc.: New Jersey, 1976; p 3393.
(34) Deutsch, E.; Root, M. J.; Nosco, D. L. In *Advances in Inorganic and Bioinorganic Mechanisms*; Sykes, A. G., Ed.; Academic Press: London, 1982; p 269.
(35) Boorman, P. M.; Chivers, T.; Mahadev, K. N.; O'Dell, B. D. *Inorg. Chim. Acta* **1976**, *19*, L35.
(36) Leonard, K.; Plute, K.; Haltiwanger, R. C.; Rakowski-DuBois, M. *Inorg. Chem.* **1979**, *18*, 3246.

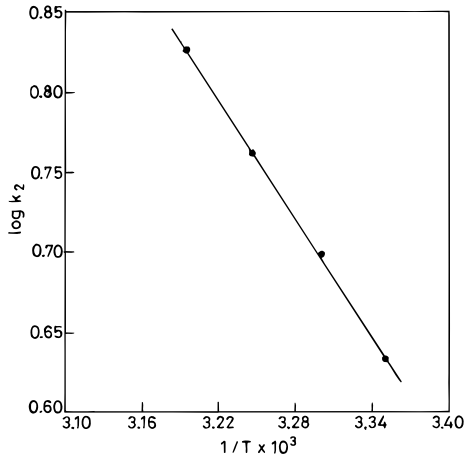

Figure 4. Eyring plot of the observed rate constants of reaction between $[Et_4N]_2[W^{VI}O(S_2)(mnt)_2]$ and Ph_3P.

Table 5. Kinetic Data for the Sulfur Atom Transfer Reaction 5 (MeCN Solution)

T, K	k_2, M^{-1} s^{-1}	$\Delta H^{\ddagger}$ kcal/mol	$\Delta S^{\ddagger}$ cal/(deg·mol)
298	4.30 (± 0.06)	5.14 (± 0.46)	−38.35 (± 1.5)
303	4.99 (± 0.03)		
308	5.785 (± 0.025)		
313	6.75 (± 0.09)		

resulted in insertion of the alkyne across Mo−S bond instead of the S−S bond.[38] In the present case, the simultaneous attack by two phosphines of WS_2 moiety can be viewed similarly.

Attempts have been made to understand the possible attack by phosphine across the W−S bond by monitoring the progress of this reaction using a time-dependent cyclic voltammetric study. This is shown in Figure 5. **3** (1×10^{-3}M in MeCN) showed an irreversible reduction peak potential at −1.45 V *vs* Ag/AgCl (supporting electrolyte, Et_4NClO_4 (0.1 M), scan rate 0.100 V s^{-1}, temperature 25 ± 1 °C). When 2 equiv of Ph_3P was added and the resultant solution was scanned after the lapse of ca. 2 min, the E_{PC} of **3** distinctly shifted to a less negative potential by 40 mV. Similar progress of the reaction between $[Bu_4N]_2[Mo^{VI}O_2(mnt)_2]$[11] and Ph_3P has been monitored cyclic voltammetrically for comparison. This reaction followed second-order kinetics. In this case, there was no change in the position of E_{PC} of the complex anion during the course of the reaction.[39] For this type of reaction the attack by phosphine on a terminal oxo group has been proposed.[40] The shift in cathodic peak potential as observed in Figure 5 thus could be the manifestation of direct attack of Ph_3P on the tungsten center, resulting in its easier reduction.

The facile reductive sulfur abstraction with Ph_3P demonstrated the importance of the kinetic aspect in atom transfer reactions. In the present case, the irreversible reduction peak potential as high as −1.45 V vs Ag/AgCl (of **3**) thus attests that such a high value does not really predict whether an atom transfer reaction will occur smoothly at ambient conditions.

Role of $[W^{IV}O(mnt)_2]^{2-}$ in the Reduction of Elemental Sulfur. The reaction between elemental sulfur and Ph_3P did not produce any Ph_3PS in MeCN after 24 h at ambient conditions. However, addition of **2** to this reaction mixture catalyzed the formation of Ph_3PS. Thus, when **2** was placed in

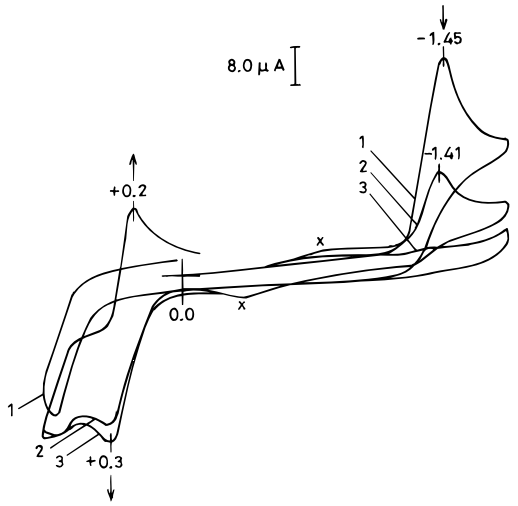

Figure 5. Cyclic voltammetric scans during the progress of the reaction between $[Et_4N]_2[W^{VI}O(S_2)(mnt)_2]$ and 2 equiv of Ph_3P. The first scan is for the pure complex. The second scan is after the addition of 2 equiv of Ph_3P with a lapse of ca. 2 min, and the third scan is 15 min after the second scan. On the positive side the appearance of a WO(IV)/WO(V) couple for the complex $[W^{IV}O(mnt)_2]^{2-}$ (formed during the progress of reaction) is observed. × marked peaks are unidentified. (For conditions, see text.)

MeCN solution containing 120 equiv of Ph_3P and 100 equiv of elemental sulfur, the resultant solution with dispersed sulfur retained the characteristic purple color of the W(IV) complex alone. Upon stirring of the solution, suspended elemental sulfur started to go into solution, and after 3 h, a clear solution was obtained. The absorption spectrum (visible range) at this stage revealed the presence of unchanged **2**. Further addition of 20 equiv of elemental sulfur and stirring for an additional 1 h dissolved the additional sulfur without any change in the absorption spectrum. Isolation of the products (*vide supra*) confirmed the formation of Ph_3PS in 98% yield in this reaction. The insolubility of elemental sulfur precluded following the catalytic rate of this reaction spectrophotometrically. No such reaction is observed in the absence of **2**.

We failed to observe any formation of H_2S from **3** in MeCN under a stream of H_2 even at a temperature of 60 °C. Furthermore, **3** was found to be stable in MeCN solution under H_2S for a prolonged time. However, when the reaction between **2** and elemental sulfur (sublimed) was done under a stream of H_2 gas (MeCN:H_2O (4:1), pH 5 with acetic acid, temperature 60 °C), the formation of H_2S did occur (tested by lead acetate as PbS). The H_2S production was visibly increased (PbS formation) with the increase in the concentration of **2** in these reactions. No such reaction is observed in the absence of **2**. The H_2S production gradually ceased, and the electronic spectrum of the resultant solution showed appreciable conversion of **2** to **3** under hydrogen. At this stage it is difficult to rationalize the entire course of this reaction. However, the initial formation of a precursor complex between **2** and elemental sulfur is likely. This sulfur adduct of **2** may be involved to react with hydrogen to produce H_2S parallel to its relatively faster conversion to **3**.

Ligand Extrusion Reaction of $[W^{IV}O(mnt)_2]^{2-}$ with MoO_4^{2-}. It has been demonstrated that molybdenum can displace tungsten from acid-treated tungsten formate dehydrogenase to form a molybdenum cofactor which can activate the *nit-1* mutants of *Neurospora crassa* for nitrate reductase, supporting that the tungsten formate dehydrogenase (W-FDH) contains molybdopterin ligation similar to that of oxomolybdoenzymes.[9] This experiment relates the ability of dithiolene containing molybdopterin extrusion from tungsten cofactor by

(37) Coucouvanis, D.; Hadjikyriacou, A.; Draganjac, M.; Kanatzides, M. G.; Ileperuma, O. *Polyhedron* **1986**, *5*, 349.
(38) Halbert, T. R.; Pan, W.-H.; Stiefel, E. I. *J. Am. Chem. Soc.* **1983**, *105*, 5476.
(39) Das, S. K. Ph. D. Thesis, IIT Kanpur, 1994.
(40) (a) Durant, R.; Garner, C. D.; Hyde, M. R.; Mabbs, F. E.; Parsons, J. R.; Richens, D. *J. Less-Common Met.* **1977**, *54*, 459. (b) Holm, R. H. *Coord. Chem. Rev.* **1990**, *100*, 183.

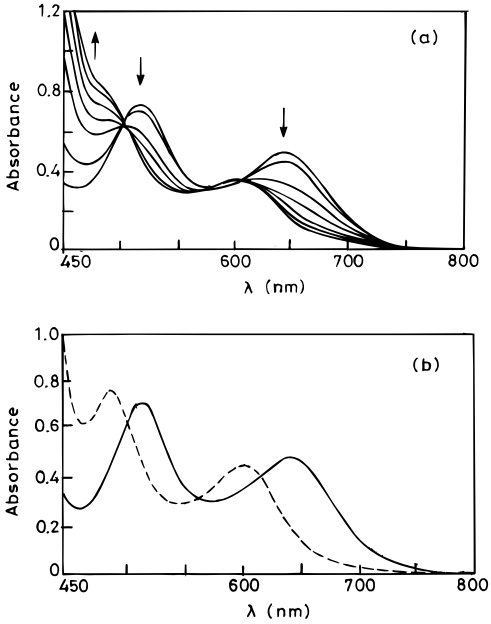

Figure 6. (a) Spectral changes for the reaction between $[Et_4N]_2[W^{IV}O(mnt)_2]$ and $Na_2MoO_4{\cdot}2H_2O$ (1:1 ratio) in MeCN:H_2O (1:1) (acetate buffer, pH ~ 5.0) at 50 °C. (b) UV−visible absorption spectra of $[Et_4N]_2[W^{IV}O(mnt)_2]$ (—) and $[Et_4N]_2[Mo^{IV}O(mnt)_2]$ (- - -).

acidified molybdate to form the molybdenum cofactor. In an attempt to model this reaction, we studied the reaction between **2** and MoO_4^{2-} in MeCN:acetate buffer in water (1:1, v/v) medium around pH 5.0 which led to the conversion (eq 7)

$$[W^{IV}O(mnt)_2]^{2-} + MoO_4^{2-} \rightarrow [Mo^{IV}O(mnt)_2]^{2-} + WO_4^{2-} \quad (7)$$

involving intermetallic electron transfer reaction with the isolation of $[Mo^{IV}O(mnt)_2]^{2-}$ (as the Et_4N^+ salt) in 65% yield (*vide supra*). The progress of this reaction (eq 7) as observed spectrophotometrically is shown in Figure 6a. For comparison, the superimposed electronic spectra comprized of $[Mo^{IV}O(mnt)_2]^{2-}$ and $[W^{IV}O(mnt)_2]^{2-}$ taken under identical conditions are shown in Figure 6b. At the initial stage of the progress of the reaction, common points of electronic spectra were at 620, 565, and 500 nm. However, during the progress of the reaction, these cutting points changed, and at the later stage of the reaction, dissociation of the free ligand, whose absorption band's tail appeared near 470 nm, was observed. It is important to comment on the two events in operation in this reaction which are the exchange of the dithiolene ligand and the intermetallic electron transfer reactions. The spectral changes (Figure 6a) clearly showed the exchange of dithiolene ligation from the tungsten to molybdenum center. To account for the electron transfer, a time-dependent EPR study was performed. Stoichiometric amounts of **2** and sodium molybdate were taken in the same media as used in the spectrophotometric study and subjected to room-temperature EPR measurements. The time-dependent EPR spectra as observed are shown in Figure 7. Within 5 min, the appearance of a weak signal with $\langle g \rangle = 1.956$ was observed, which after 15 min stayed with the appearance of another broad signal with $\langle g \rangle = 1.92$. With the progress of time, the intensity of both of the signals increased, and after 75 min, the signal at $\langle g \rangle = 1.956$ started to decrease but the signal at $\langle g \rangle = 1.92$ gradually became more strong. After 3 h, the signal with $\langle g \rangle = 1.956$ completely disappeared and the intensity of the signal with $\langle g \rangle = 1.92$ attained maximum intensity which on prolonged standing also started decreasing and finally became EPR silent after 36 h. This EPR experiment clearly demonstrates that reaction (eq 7) involves stepwise one-

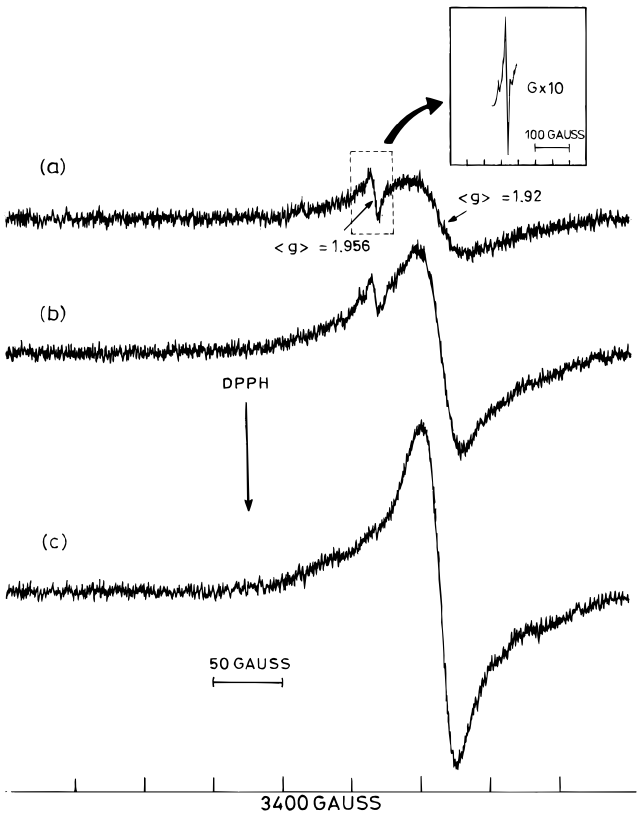

Figure 7. Time-dependent EPR (X-band) spectra of the reaction mixture of $[Et_4N]_2[W^{IV}O(mnt)_2]$ and MoO_4^{2-} (1:1 ratio) in MeCN:H_2O (1:1, pH 5.0, acetate buffer) at 25 °C: (a) after 15 min, (b) after 45 min, and (c) after 180 min (time constant 0.032 s). Inset: time constant 1.0 s to show ^{183}W hyperfine splitting ($\langle A \rangle \approx 50$ G).

electron transfer reactions. **2** in CH_2Cl_2 was chemically oxidized by 1 equiv of iodine to the corresponding EPR active W(V) species as shown in Figure 8a with $\langle g \rangle = 1.956$. Addition of an excess of $[Ph_3PNPPh_3]Cl$ to this species, $[W^{V}O(mnt)_2]^{1-}$, in CH_2Cl_2 resulted in one more EPR signal with $\langle g \rangle = 1.895$ in addition to the signal with $\langle g \rangle = 1.956$ (Figure 8b). The appearance of an EPR signal with a lower g value is indicative of Cl^- coordination to tungsten(V) as has been observed for the corresponding molybdenum complexes.[11] In the catalytically inactive, tungsten-substituted sulfite oxidase, the appearance of $\langle g \rangle = 1.89$ for the W(V) species[41] is very close to that of W(V)oxo−chloro complex. It is interesting to note that the dithiolene sulfur donors are comparable to thiolate sulfur donors in their effect on Mo(V) g values.[11] This is not true for the corresponding W(V) systems where, for $[W^{V}O(SPh)_4]^-$, $\langle g \rangle = 1.936$[42] suggests more delocalization with dithiolene ligation or with benzenedithiolate.[13] In the case of molybdenum, the Mo(V) oxo−chloro complex[11] is completely formed in the presence of excess of Cl^-, whereas for the tungsten system, the penta- and hexacoordinated W(V) species remained in equilibrium under identical conditions. On the basis of these results, the EPR signal at $\langle g \rangle = 1.956$ (Figure 7) showing characteristic ^{183}W (14.4%, $I = {}^1/_2$) isotope splitting in the ligand extrusion reaction is assigned for $[W^{V}O(mnt)_2]^{1-}$. The signal centered at $\langle g \rangle = 1.92$ (Figure 7) which later gained intensity at the expense of the disappearance of $[W^{V}O(mnt)_2]^{1-}$ should then be for a tungsten(V) species in higher coordination form because the characteristic hyperfine splitting for Mo(V) was not observed with this signal and the broad nature of the signal

(41) (a) Rajagopalan, K. V. In *Molybdenum and* Molybdenum *Containing Enzymes*; Coughlan, M. P., Ed.; Pergamon Press: Oxford, U.K., 1980; p 243. (b) Johnson, J. L.; Rajagopalan, K. V. *J. Biol. Chem.* **1976**, *251*, 5505.

(42) Hanson, G. R.; Brunette, A. A.; McDonell, A. C.; Murray, K. S.; Wedd, A. G. *J. Am. Chem. Soc.* **1981**, *103*, 1953.

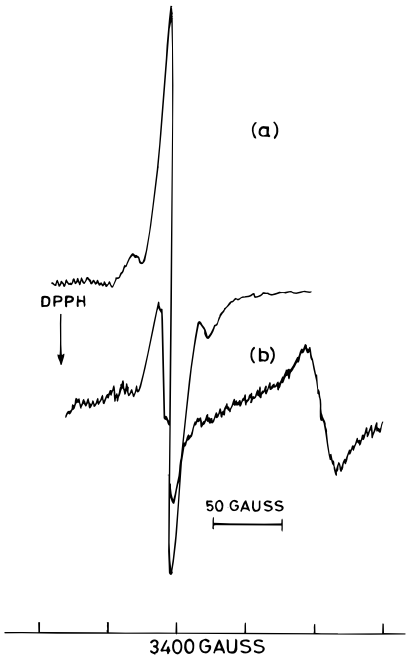

Figure 8. (a) EPR spectrum (X-band) of $[W^{V}O(mnt)_2]^{1-}$ in CH_2Cl_2 formed by the reaction between equivalent amounts of $[Et_4N]_2[W^{IV}O(mnt)_2]$ and iodine (^{183}W $\langle A\rangle = 53$ G. (b) same solution spectrum in the presence of $[Ph_3PNPPh_3]Cl$.

with $\langle g\rangle = 1.92$ was similar to that observed with the iodine-oxidized chloro-coordinated W(V) species (Figure 8b). The extra stability of this signal is not surprising because, under sulfur ligation, the EPR signal of a oxotungsten(V) species is reported to be stable for a long duration of time.[15c] The nonappearance of any EPR active Mo(V) species may be due to its presence as a dimeric EPR inactive intermediate $Mo_2(V)$ form or its susceptibility to disproportionation reactions under the reaction conditions.[11]

Interestingly identification of an EPR active W(V) center with the expected isotopic splitting has been observed in the tungsten-substituted form of *M. wolfei* molybdoenzyme, formylmethanofuran dehydrogenase (FMDHI), under aerial oxidation.[43] The ligation around tungsten of this species is not yet known.

Aldehyde Oxidase Analogue Activity of 3. $[Et_4N]_2[W^{VI}O_2(mnt)_2]$ (**1**) contains credible coordination units in relevance to the inactive RTP form of the tungsten protein of *P. furiosus*. Under sulfiding conditions, $[Et_4N]_2[W^{VI}O(S_2)(mnt)_2]$ (**3**) is formed, retaining an oxotungsten(VI) moiety. Both **1** and **3** under reduction yield $[Et_4N]_2[W^{IV}O(mnt)_2]$ (**2**). The reaction of **1** with H_2S ultimately yielded **2** and **3** with a reactive intermediate possibly containing the $\{W^{VI}OS\}$ or $\{W^{VI}O(SH)_2\}$ moiety. Thus, to test the aldehyde oxidase activity, reactions were carried out with **1**, **1** with H_2S and with **3**, using formaldehyde and crotonaldehyde as substrates.

1 with an excess of crotonaldehyde or formaldehyde in MeCN containing H_2O (5%, v/v) did not show any formation of **2** at room temperature, and at a temperature of 45 °C, the complex gradually decomposed. A similar reaction under H_2S with and without aldehyde at 45 °C yielded predominantly **2**, and any difference in these reactions (with and without aldehyde) could not be ascertained with certainty except the additional formation of thio derivatives of aldehydes under H_2S.

When an MeCN containing a H_2O (5%, v/v) solution of **3** (1.0 mM) was treated with an excess of formaldehyde (pH 6.2, adjusted by using Et_3N) and kept for 2 days at room temperature, **2** was formed in 40% as observed spectrophotometrically with a drop of pH to 6.0. Similarly a mM solution of **3** in MeCN−H_2O (pH 7.9, adjusted by using Tris buffer) with an excess of crotonaldehyde on standing overnight at 45 °C showed the formation of **2** in 20% yield as observed by spectrophotometry. A prolonged reaction (4 days) between **3** and excess crotonaldehyde in CH_2Cl_2 showed the conversion of **3** to **2** along with the formation of $[W^{IV}(mnt)_3]^{2-}$ (observed by spectrophotometry). The formation of $[W^{IV}(mnt)_3]^{2-}$ was found to be pH dependent (more at lower pH) and also caused by the use of water-free solvents. The fate of the coordinated S_2^{2-} (of **3**) in these reactions could not be directly identified. However, the formation of thio derivatives of aldehydes is a strong possibility because of the presence of a characteristic odor which could even be identified under the presence of an excess of crotonaldehyde. From the solution (reaction mixture) the crotonic acid was identified by gas chromatography (retention time peak, 1.41 (crotonic acid), 0.97 (crotonaldehyde), 0.79 (CH_2Cl_2)). Regarding the formation of $[W^{IV}(mnt)_3]^{2-}$, the protonation of $[W^{IV}O(mnt)_2]^{2-}$ may be the reason at lower pH (*vide supra*). When reactions were carried out in dry acid-free CH_2Cl_2 solvent in a colored flask to prevent photodissociation of CH_2Cl_2, the formation of $[W^{IV}(mnt)_3]^{2-}$ was not due to protonation by the formed crotonic acid, as checked by control experiments. This may be due to the formation of unstable intermediate $\{W^{IV}(S_2)(mnt)_2\}^{2-}$ after initial oxo transfer from **3**, which on hydrolysis should yield **2** and in the absence of water probably rearranged to yield $[W^{IV}(mnt)_3]^{2-}$. On the basis of these observations, a working scheme for these reactions is shown (Scheme 1).

Scheme 1

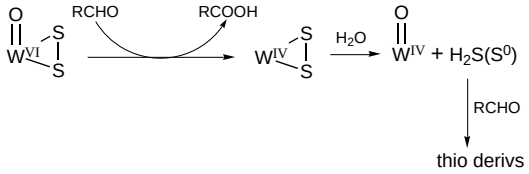

At this stage we are not sure about the disulfido ligation of tungsten in an active AOR enzyme. The release of elemental sulfur may participate to regenerate **3** from **2** (*vide supra*). The reoxidation of the reduced tungsten center of the native enzyme involves ferredoxin centers. The electronic effect of the WS_2 moiety may be simulated by the coordination of two cysteinyl thiolates in adjacent positions of the W^{VI} center in the native enzyme with partial disulfide bond formation as suggested by Stiefel for oxomolybdoenzymes.[44] The enzymatic oxo transfer reaction may then involve a similar heptacoordinated $\{W^{VI}O(SR)_2\}$ catalytic center followed by the hydrolysis of a $\{W-(SR)_2\}$ group to incorporate terminal oxo ligation to the W(IV) center with the release of labile cysteinyl −SH groups similar to that shown in Scheme 1. This may account for the reactivity difference between the inactive RTP and active AOR forms of the protein. However, if there is similarity between the Mo site of the active oxosulfido form of purine hydroxylases and the W site of active AOR enzyme, then the involvement of at least one inorganic sulfido group coordinated to the tungsten center is possible. This should respond to the established cyanolysis reaction of the molybdenum system.[45] Interestingly **3** responds to such a type of reaction. The AOR enzyme of *P. furiosus* with a molecular weight 85 kD contains seven cysteine residues, approximately the same number of iron atoms, and five atoms of inorganic sulfide.[2] The recent report of the X-ray structure of AOR demonstrates the presence of a Fe_4S_4 cluster

(43) Schmitz, R. A.; Albracht, S. P. J.; Thauer, R. K. *FEBS Lett*. **1992**, *309*, 78.

(44) Stiefel, E. I. In *Molybdenum and Molybdenum Containing Enzymes*; Coughlan, M. P., Ed.; Pergamon Press: Oxford, U. K., 1980; p 43.

(45) (a) Dixon, M.; Keilin, D. *Proc. R. Soc. B* **1936**, *119*, 159. (b) Massey, V.; Edmondson, D. E. *J. Biol. Chem*. **1970**, *245*, 6595.

with four-coordinated cysteine ligands near the tungsten cofactor in each AOR subunit. However, for the tungsten cofactor, besides four sulfur ligation from two molybdopterin ligands, the other coordination sites were suggested to be oxo or glycerol (or both) ligation. The proposed possible interaction of glycerol present in the protein storage buffer with the tungsten center of AOR[10] thus precluded the confirmation of the proposed W−SH ligation.

Conclusion

The active site of the hyperthermophilic tungsten protein of *P. furiosus* AOR enzyme is ligated by two dithiolate type of ligands (from two molybdopterins) and at least one terminal oxo group[10] with the proposed involvement of another sulfhydryl group ligation.[2b] The inactive RTP form of AOR enzyme contain a *cis* dioxo grouping with similar dithiolene coordination.[6,10] Complexes **3** and **1** also contain similar coordination around the tungsten center with the attachment of a *dihapto* sulfido group in **3** instead of the proposed −SH coordination.

The model reaction between **1** and DTT or PhSH led to the reduction of the tungsten center of **1** with the formation of **2** and with the oxidation of thiols. Redox reactions between **1** and thiols, H_2S or $S_2O_4^{2-}$, several model reactions involving analogue oxo transfer reactions of DMSO reductase, and oxo transfer reaction in native DMSO reductase are viewed as internal electron transfer between two bound redox partners present in the form of precursor or enzyme−substrate complexes. This relates the importance of kinetically controlled conditions over real reduction potential data of unbound redox partners like the free enzyme and the free substrate.

The ready protonation of the oxo group in **2** may relate to the extrinsic pH effect of reduced W-FDH and *E. coli* nitrate reductase.[46,47]

The metal exchange reaction between **2** and MoO_4^{2-} is similar to *in vitro* reconstitution of the molybdenum cofactor using reduced W-FDH.[9] The model reaction demonstrates dithiolene extrusion involving stepwise one-electron transfer from W(IV) to Mo(VI).

Interestingly, obligately anaerobe *P. furiosus* grows in a sulfur-rich environment under high-temperature conditions, and elemental sulfur stimulates its growth by disposing of the catabolite, H_2, in the form of H_2S.[2] The incorporation of tungsten into the AOR enzyme from the available form of tungsten should be an oxothio derivative like $WO_2S_2^{2-}$ or WOS_3^{2-} rather than WO_4^{2-} under such sulfiding conditions. The reactions between $WO_2S_2^{2-}$ or WOS_3^{2-} and mnt^{2-} invariably yielded a mixture of **2** and **3**. **1** under H_2S atmosphere also yielded the same products. The failure to isolate any bis-dithiolene coordinated complex containing either the $\{W^{VI}OS\}$ or $\{W^{VI}(OSH\}$ moiety, in the present study, does not prove the nonexistence of such moieties in the active AOR enzyme. Considering high-temperature and reducing H_2S atmospheric conditions, a W═S or W−SH group in the resting W^{VI} form of AOR enzyme is highly unlikely. Complex **3** demonstrates its ease of formation under sulfiding conditions especially by oxidative addition of elemental sulfur. The solution stability of **3** under H_2 or H_2S, its reaction with thiophiles like PhSH to yield **2**, and finally its reactivity toward crotonaldehyde to yield **2** and crotonic acid firmly establish the model behavior of an active AOR enzyme. The working Scheme 1 presents the participation of H_2O to yield **2** with the protonation of S_2^{2-} resulting in $H_2S + S^0$. This H_2S reacts with excess aldehyde. The available elemental sulfur may function as an electron acceptor to regenerate **3** from **2**.

Since tungsten-containing hyperthermophilic archaea are considered to be the most primitive organisms known at present,[1] it is speculated that the earliest life forms were also tungsten dependent.[2] The ubiquitous presence of molybdenum enzymes catalyzing oxo transfer reactions in mesophilic organisms where tungsten shows antagonism must be related to the difference in the chemistry between tungsten and molybdenum. Interestingly, moderately thermophilic organisms with formate dehydrogenase activity can incorporate tungsten as well as molybdenum. Besides the thermal effect, hyperthermophiles are strict anaerobes compared to molybdenum-dependent mesophilic systems. In all of these molybdenum- and tungsten-dependent enzymes, the redox states involved in a catalytic cycle are 6+ and 4+. For the 4+ oxidation state, the oxotungsten(IV) complex **2** is very oxygen sensitive, whereas the corresponding oxomolybdenum(IV) complex is reasonably stable under aerobic condition.[11] Furthermore, oxo complexes of molybdenum(VI) are thermally less stable compared to the corresponding tungsten(VI) complexes. The kinetic sluggishness of tungsten(VI) complexes does require higher temperature to perform reactions which are done by the corresponding molybdenum complexes at room temperature. Lastly, most of the hyperthermophiles require hot sulfiding conditions for significant growth. In such an unusual environment, tungsten, not molybdenum, can remain in the 6+ oxidation state that is essential for catalyzing oxo transfer reactions.

Acknowledgment. We thank Professor P. K. Bharadwaj for help in the X-ray structure analysis. We are grateful to Professors D. C. Rees and M. W. W. Adams for sending structural information on the tungsten−pterin cofactor of *P. furiosus* AOR enzyme prior to publication. Our report has benefited from reprints and preprints kindly supplied by Professors M. W. W. Adams and J. H. Enemark. Support of this work and of the National X-ray Diffractometer facility at IIT Kanpur by the Department of Science and Technology, Government of India, is gratefully acknowledged. This article is dedicated to Professor Animesh Chakravorty, on the occasion of his 60th birthday.

Supporting Information Available: Listings of thermal parameters of non-hydrogen atoms, calculated hydrogen atom parameters, bond lengths, and bond angles and figures showing spectral changes in the reactions of **2** and Cl_3COOH, **1** and $S_2O_4^{2-}$, **1** and H_2S/Ph_3P, **3** and Ph_3P, and **3** and formaldehyde (17 pages); listing of structure factors for $[Ph_4P]_2[W^{VI}O_2(mnt)_2]\cdot 2H_2O$, **2** and **3** (104 pages). This material is contained in many libraries on microfiche, immediately follows this article in the microfilm version of the journal, can be ordered from the ACS, and can be downloaded from the Internet; see any current masthead page for ordering information and Internet access instructions.

JA9511580

(46) Cramer, S. P.; Liu, C.-L.; Mortenson, L. E.; Spence, J. T.; Liu, S.-M.; Yamamoto, I.; Ljungdhal, L. G. *J. Inorg. Biochem.* **1985**, *23*, 119.

(47) Cramer, S. P.; Solomonson, L. P.; Adams, M. W. W.; Mortenson, L. E. *J. Am. Chem. Soc.* **1984**, *106*, 1467.